ResearchGate

See discussions, stats, and author profiles for this publication at: https://www.researchgate.net/publication/7373463

Evaluation and Optimization of the Conditions for an Improved Ferulic Acid Intercalation into a Synthetic Lamellar Anionic Clay

ARTICLE *in* PHARMACEUTICAL RESEARCH · APRIL 2006

Impact Factor: 3.42 · DOI: 10.1007/s11095-005-9394-y · Source: PubMed

CITATIONS
3

READS
23

7 AUTHORS, INCLUDING:

Paolo Blasi
University of Camerino
62 PUBLICATIONS **1,317** CITATIONS
SEE PROFILE

Stefano Giovagnoli
Università degli Studi di Perugia
67 PUBLICATIONS **1,385** CITATIONS
SEE PROFILE

Luana Perioli
Università degli Studi di Perugia
95 PUBLICATIONS **1,926** CITATIONS
SEE PROFILE

Carlo Rossi
Università degli Studi di Perugia
100 PUBLICATIONS **2,273** CITATIONS
SEE PROFILE

Available from: Stefano Giovagnoli
Retrieved on: 24 January 2016

Pharmaceutical Research, Vol. 23, No. 3, March 2006 (© 2006)
DOI: 10.1007/s11095-005-9394-y

Research Paper

Evaluation and Optimization of the Conditions for an Improved Ferulic Acid Intercalation into a Synthetic Lamellar Anionic Clay

Aurélie Schoubben,[1] Paolo Blasi,[1] Stefano Giovagnoli,[1] Morena Nocchetti,[2] Maurizio Ricci,[1] Luana Perioli,[1] and Carlo Rossi[1,3]

Received June 16, 2005; accepted November 3, 2005

Purpose. The aim of the study is to optimize the intercalation conditions of ferulic acid (FERH), an antioxidant compound, into Mg–Al–hydrotalcite for a safe skin photoprotection.
Methods. The intercalation products were prepared incubating hydrotalcite (HTlc) in aqueous solutions of FERH sodium salt at different temperatures over 4 and 8 days. Quantitative determination of intercalated FERH was performed by thermogravimetric analysis and morphology by scanning electron microscopy (SEM). FERH stability study was carried out at different pHs and temperatures. FERH was analyzed by reversed phase–high-performance liquid chromatography. Response surface methods (RSMs) were used to assess optimal intercalation conditions and FERH stability.
Results. In all intercalation products, FERH content was found to be about 48% w/w except when the intercalation process was carried out at 52°C for 8 days and at 60°C for both 4 and 8 days, which resulted to be 40.39, 39.99, and 34.99%, respectively. The RSM designs showed that intercalation improvement can be achieved by working at pH 6, at temperatures below 40°C, and over 4 days of incubation.
Conclusions. The optimal conditions for a proper FERH intercalation were assessed. The development of a new optimized protocol may improve HTlc–FER complex performances and safety by augmenting dosage and reducing the presence of harmful reactive species in the final formulation.

KEY WORDS: ferulic acid; intercalation; Mg–Al hydrotalcite; optimization; stability.

INTRODUCTION

FERH, 4-hydroxy-3-methoxycinnamic acid (Fig. 1), is a substance found in seeds and leaves of most plants, especially in the brans of grasses such as wheat, rice, and oats. Its valuable properties owe to its radical scavenging activity, which can be enhanced by exposure to ultraviolet (UV) light; this feature suggests that it might be helpful in protecting skin from sun damage (1–5). In a previous work (6), FERH was intercalated, as a dissociated form (FER), in hydrotalcite chloride (HTlc–Cl). HTlc–Cl is an anionic clay characterized by positively charged metal hydroxide sheets with anions located interstitially. HTlc has been used as catalyst (8), catalyst support (9), adsorbent (10), pharmaceutical vector (11), for the preparation of modified release formulations (12), and as a cosmetic formulation stabilizer (13). FER intercalation in HTlc (6) proved to be useful in protecting it from degradation because of irradiation and therefore potentially in enhancing FERH sunscreen properties in the region around 300 nm.

FERH can be degraded in the presence of bacteria or fungi (14–16) and easily undergoes decarboxylation and oxidation (17–21). Furthermore, it is susceptible to environmental factor modifications, especially temperature and pH, which have great importance on the intercalation process (5,22). The presence of FERH degradation products may affect the proper and effective intercalation of the molecule, as these byproducts may compete with FERH during the inclusion process in HTlc–Cl. In addition, the presence of degradation products may favor formation of radicals and other harmful reactive species hence causing dangerous side effects upon application on skin. In light of these considerations, the present work was aimed at the investigation of FERH stability under different environmental conditions to improve the intercalation process and to assess the optimal conditions for HTlc–FER fabrication. When possible, the presence of potentially interfering degradation products in the intercalation complex was evaluated. Degradation products were investigated by assaying the intercalated compounds and supernatants using a reversed phase–high-performance liquid chromatography (RP-HPLC) technique.

Investigation of FERH stability was carried out at pH 2.2, 4, and 7.4 and in the temperature range of 4–60°C. HTlc–FER complexes were characterized by X-ray diffraction, thermogravimetry, and scanning electron microscopy (SEM). Temperature and pH effects on stability and time and temperature on intercalation were assessed by means of

[1] Dipartimento di Chimica e Tecnologia del Farmaco, University of Perugia, 06123 Perugia, Italy.
[2] Dipartimento di Chimica, University of Perugia, 06123 Perugia, Italy.
[3] To whom correspondence should be addressed. (e-mail: cfrossi@unipg.it)

0724-8741/06/0300-0604/0 © 2006 Springer Science + Business Media, Inc.

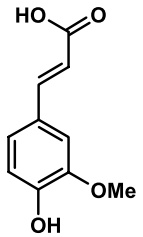

Fig. 1. FERH structure.

two response surface methods (RSMs). This approach may provide useful information for the development of a new protocol for FERH intercalation in HTlc–Cl matrices to increase the amount of intercalated FERH and to avoid the presence of potentially harmful reactive species in the final product.

MATERIALS AND METHODS

Materials

FERH and $AlCl_3{\cdot}6H_2O$ were purchased from Fluka (Milan, Italy). $MgCl_2{\cdot}6H_2O$, urea, and acetonitrile for HPLC were obtained from Baker (Deventer, Holland). 4-Vinylguaiacol, sodium phosphate, acetic acid, and lactic acid were acquired from Sigma Aldrich (Milan, Italy). Water Plus for HPLC was provided by Carlo Erba (Rodano, Italy). Other chemicals and solvents were of reagent grade and were used without further purification.

HTlc–Cl Preparation

The HTlc–Cl was obtained starting from its carbonate form. The Mg–Al–HTlc–CO_3 was prepared by adding solid urea to a 0.5 M $MgCl_2/AlCl_3$ water solution. Urea/Mg + Al and Al/Mg + Al were in the molar ratio of 3.3 and 0.33, respectively. The hydrolysis of urea, inducing slow pH increase, led to the precipitation of metals in a well-crystallized HTlc carbonate form (7). The obtained solid was recovered, washed with water to eliminate chlorides, and stored in a desiccator under vacuum at room temperature. Quantification of magnesium and aluminum was accomplished by ethylenediaminetetraacetic acid titration of a HTlc–CO_3 aqueous solution (50 ml) obtained by dissolving the product with a proper amount of HCl 0.1 N at pH < 5.

Pure crystalline Mg–Al–HTlc–Cl was obtained by $CO_3{}^{-2}/Cl^-$ ion exchange upon titration with a dilute HCl solution (23).

Intercalation of FERH into HTlc–Cl

HTlc–Cl (0.303 g) was suspended in 25 ml of a degassed aqueous solution of ferulate sodium salt (FER^-Na^+ 0.546 g), obtained by adding stoichiometric equivalents of carbon-dioxide-free 0.1 N NaOH solution to FERH (Cl^-/FER^- molar ratio 1:2). Intercalation was performed at six different temperatures (25–32–37–45–52–60°C), 140 rpm over 4 and 8 days in a Gallenkamp orbital incubator INR 2000 (Gallenkamp, UK). The reaction was carried out protecting samples from light and under nitrogen atmosphere to protect reagents from oxidation.

HTlc–FER was centrifuged in an ALC centrifuge 4236A (ALC, Milan, Italy) at 4000 rpm for 5 min and was washed first with degassed water, then with ethanol 95%, and finally with degassed water. The product was dried in a desiccator under vacuum. The supernatant obtained after the first centrifugation was analyzed by RP-HPLC to evaluate the presence of FERH degradation products.

Characterization of the Intercalated Product

HTlc–FER was analyzed by X-ray powder diffraction (XRPD) with a computer-controlled PW 1710 Philips diffractometer (Philips, Eindhoven, Netherlands), using the Ni-filtered Cu Kα radiation. Quantitative determination of intercalated FERH was performed by thermogravimetric analysis (TGA) with a Stanton-Redcroft STA 780 thermoanalyzer at a heating rate of 5°C min^{-1} under airflow. Analyses were performed in triplicate, and the error was expressed as standard deviation.

Morphology of HTlc–FER intercalation compounds was determined by SEM using a Philips XL30 microscope. Pictures of blank HTlc–Cl matrix were also recorded to evaluate the effect of intercalation on the final product.

RP-HPLC Analysis

Reversed phase–high-performance liquid chromatography analyses were carried out by means of a HP 1050 Series chromatograph (Hewlett Packard, Waldbronn, Germany) equipped with a spectrophotometer HP 1050 Series detector (Hewlett Packard) set at 310 nm, using a Waters C18 column (100 Å, 300 × 3.9 mm; Waters, Milan, Italy). Elutions were performed in an isocratic manner (flow rate 1 ml/min) with a mixture of water–CH_3COOH (pH 3)/acetonitrile (66:34, v/v).

Column, mobile phase, and samples were equilibrated at room temperature. The calibration curves were drawn with six solutions in the concentration range of 2–12 μg/ml. Measurements were performed in four replicates, and the error was expressed as standard deviation.

FERH Stability Studies

FERH stability was tested at three different pHs (2.2, 4, and 7.4) and at three different temperatures (4, 37, and 60°C). Three buffers were used according to the pH needed: 0.1 M phosphate buffer pH 7.4, 0.1 M acetic buffer pH 4, and 0.1 M lactic buffer pH 2.2. FERH solutions, with a theoretical concentration of 0.2 mg/ml, were prepared in triplicate using the aforementioned buffers. Samples of 250 μl were withdrawn at predetermined time intervals and were analyzed by RP-HPLC. Particular care was taken to avoid FERH light-mediated degradation.

The data obtained were used to build an Arrhenius plot:

$$\log k = \log A - E_a/2.303\,k_b T \qquad (1)$$

where A is an unknown nonthermal constant, E_a is the activation energy of the reaction, k_b is the Boltzmann's constant, and T is the absolute temperature (Kelvin).

The Arrhenius rate constants (k) were thus calculated at each pH and temperature value. The set of k's was employed

for the evaluation of FERH stability conditions and the relative effects of pH and temperature.

Assessment of Time and Temperature Effects on FERH Intercalation

Response surface method was employed to analyze temperature and time effects on FERH intercalation. Two factors were chosen, namely, time (A) and temperature (B), whereas the response to be evaluated was FERH % of intercalation. Time was varied over two levels (4 and 8 days) and temperature over six levels (25, 32, 37, 45, 52, and 60°C) as already reported in Intercalation of FERH into HTlc–Cl and in Table I. A D-optimal design was built, and a quadratic polynomial model was employed:

$$Y = b_0 + b_1X_A + b_2X_B + b_5X_A^2 + b_6X_B^2 + b_3X_AX_B + \varepsilon \quad (2)$$

A and B are the factors, b_i are the coefficients estimating main effects and interactions, and ε is the residual error of the model.

Twelve design points were employed in the RSM. Diagnostic and analysis of variance (ANOVA) statistics were performed to assess model adequacy. Using the reported model, a contour plot of % FERH intercalated was built vs. time and temperature. This procedure was useful to evaluate time and temperature influences on FERH intercalation into HTlc–Cl.

Assessment of pH and Temperature Effects on FERH Stability

To establish the extent of temperature and pH effects on FERH degradation, a RSM was employed, as described earlier in Assessment of Time and Temperature Effects on FERH Intercalation. The two factors chosen were temperature (A) and pH (B), whereas the response to be evaluated was the FERH degradation rate constant (k). k was calculated from the Arrhenius plot as previously reported. The factors were varied over three levels corresponding to the three values of temperature (4, 37, and 60°C) and pH (2.2, 4, and 7.4). A D-optimal design was built by augmenting a 2^2 full factorial design, previously obtained by varying temperature and pH over their maximum and minimum levels. In such a way, curvature was evaluated by introducing checkpoints represented by the temperature mid-level (37°C) at all three pH levels (2.2, 4, and 7.4).

A general polynomial model was employed as shown by:

$$Y = b_0 + b_1X_A + b_2X_B + b_5X_A^2 + b_6X_B^2 + b_3X_AX_B + b_7X_A^2X_B + \ldots + \varepsilon \quad (3)$$

A and B are the factors, b_i are the coefficients estimating main effects and interactions, and ε is the residual error of the model.

Nine replicates for each level were performed, and 36 design points resulted in the 2^2 factorial design. These points were employed for the analysis in the D-optimal response surface design upon addition of checkpoints. Diagnostic and ANOVA statistics were applied to assess performance and reliability of the model obtained. Eventually, a k surface

Table I. FERH Intercalation in HTlc Clay Performed Under Different Periods of Time and Temperatures

	Intercalation period			
	4 Days		8 Days	
Temperature (°C)	Formula	FER content (% w/w) ± SD[a]	Formula	FER content (% w/w) ± SD[a]
25	$[Mg_{0.62}Al_{0.38}(OH)_2]$ $FER_{0.356}Cl_{0.024}{\cdot}0.90H_2O$	47.6 ± 0.9	$[Mg_{0.62}Al_{0.38}(OH)_2]$ $FER_{0.374}Cl_{0.006}{\cdot}1.03H_2O$	48.1 ± 0.2
32	$[Mg_{0.62}Al_{0.38}(OH)_2]$ $FER_{0.354}Cl_{0.026}{\cdot}0.86H_2O$	47.5 ± 0.7	$[Mg_{0.62}Al_{0.38}(OH)_2]$ $FER_{0.38}{\cdot}0.90H_2O$	49.3 ± 0.5
37	$[Mg_{0.62}Al_{0.38}(OH)_2]$ $FER_{0.365}Cl_{0.015}{\cdot}0.98H_2O$	47.6 ± 0.9	$[Mg_{0.62}Al_{0.38}(OH)_2]$ $FER_{0.362}Cl_{0.018}{\cdot}0.85H_2O$	48.2 ± 0.9
45	$[Mg_{0.62}Al_{0.38}(OH)_2]$ $FER_{0.378}Cl_{0.002}{\cdot}0.86H_2O$	49.4 ± 0.6	$[Mg_{0.62}Al_{0.38}(OH)_2]$ $FER_{0.38}{\cdot}0.97H_2O$	48.9 ± 0.6
52	$[Mg_{0.62}Al_{0.38}(OH)_2]$ $FER_{0.356}Cl_{0.024}{\cdot}0.75H_2O$	48 ± 2	$[Mg_{0.62}Al_{0.38}(OH)_2]$ $FER_{0.258}Cl_{0.122}{\cdot}0.55H_2O$	40.4 ± 0.8
60	$[Mg_{0.62}Al_{0.38}(OH)_2]$ $FER_{0.299}Cl_{0.081}{\cdot}0.55H_2O$	40 ± 1	$[Mg_{0.62}Al_{0.38}(OH)_2]$ $FER_{0.201}Cl_{0.179}{\cdot}0.36H_2O$	35 ± 1

HTlc: Hydrotalcite.
[a] $n = 3$.

response plot was generated to monitor its modifications with pH and temperature. This procedure was useful to optimize the conditions for FERH intercalation into HTlc–Cl and to evaluate the influence of pH and temperature on FERH stability.

Evaluation of FERH Degradation

Further qualitative studies were performed on the solutions used to investigate FERH stability and the supernatants collected during the intercalation process to highlight the presence of possible degradation products. HPLC analyses were carried out on samples used for the stability study and on the intercalation products in the attempt to reveal known byproducts caused by FERH chemical transformation. For this purpose, HPLC profiles were compared to those obtained from known degradation products, such as 4-vinylguaiacol (14).

RESULTS AND DISCUSSION

Characterization of the Intercalated Compounds

The HTlc matrix was prepared as chloride form to favor ion exchange process (23); HTlc–Cl composition resulted: $Mg_{0.62}Al_{0.38}(OH)_2 \cdot Cl_{0.38} \cdot 0.56H_2O$. HTlc–Cl was then converted into HTlc–FER form according to the procedure described in Intercalation of FERH into HTlc–Cl.

XRPD was used to confirm FERH intercalation. As shown in Fig. 2, space between layers increased from 7.8 Å (24) to 17.7 Å in each preparation as a consequence of FERH intercalation (25).

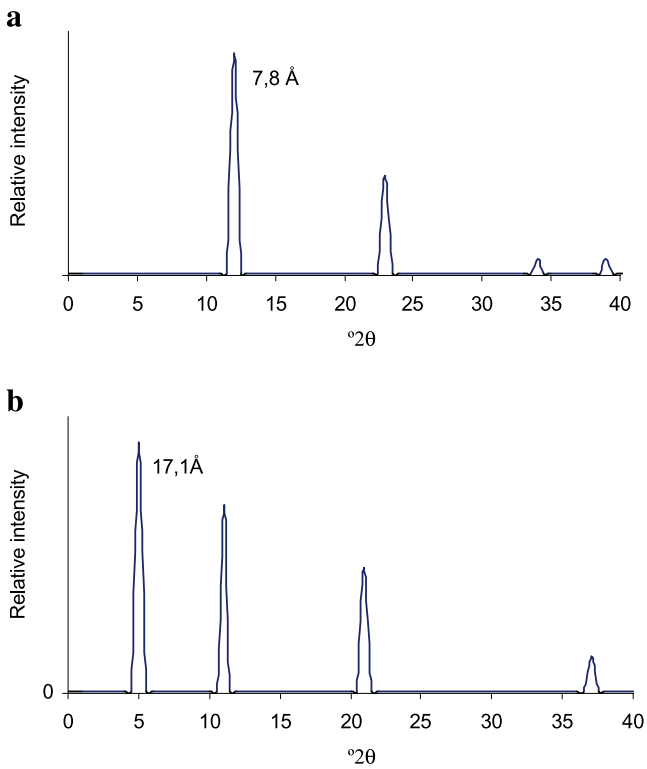

Fig. 2. X-ray powder diffraction characterization of HTlc–Cl (A) and HTlc–FER (B).

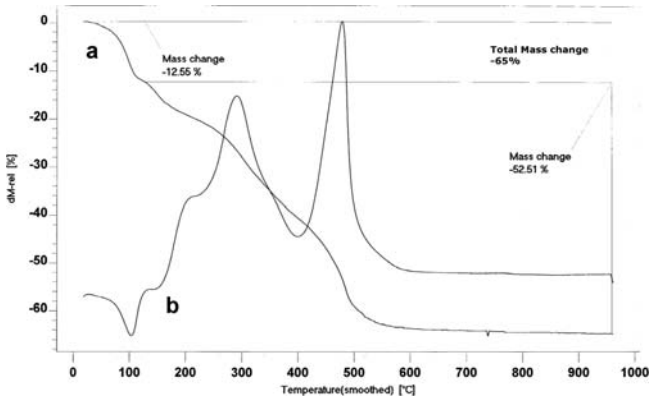

Fig. 3. HTlc–FER thermogravimetric analysis reporting (a) % weight loss and (b) thermal transition curve.

TGA profiles (Fig. 3) had very similar patterns and were characterized by three stages. The first stage showed a broad endotherm at 100°C because of loss of both adsorbed and interlayer water molecules. The two exothermic bands at 200–350 and at 400–600°C are mainly a result of FERH decomposition and of an outdiffusion of FERH as well as the dehydroxylation of the host layers, respectively. The product obtained at 1000°C consisted only of a mixture of MgO and Al_2O_3.

In light of these observations, HTlc–FER exact formula and FERH content were then calculated (Table I).

The intercalation yield of FERH in HTlc ranged from 35 to about 49%. It was slightly increased at low temperatures and at longer times (8 days), whereas comparable results were obtained at higher temperatures and shorter times (4 days). The intercalation compounds obtained showed a homogeneous morphology with lamellar layer structures (Fig. 4A and B). Moreover, intercalation did not affect morphology as blank matrix, and intercalation compounds did not show evident differences in shape and size.

Effect of Factors on Intercalation and FERH Stability

The data obtained from the intercalation study were analyzed by a D-optimal design to evaluate intercalation efficiency susceptibility to the working conditions employed. A reduced quadratic model was obtained:

$$Y = 48.37 - 0.96X_A - 4.60X_B - 5.86X_B^2 - 2.08X_AX_B \quad (4)$$

Diagnostic and ANOVA analyses showed model adequacy with significant terms and large F values (Table II). A good agreement was observed between predicted and adjusted r^2 (data not shown).

Time (factor A) did not have an effect as high as temperature (factor B) on intercalation, as it was shown by the small second coefficient in Eq. (4) and the small F value in Table II. Nevertheless, it had a large effect when associated to temperature as reported by the highly significant AB interaction term. A region of optimality in which FERH intercalation was increased to about 49% was outlined by analyzing the contour plot generated from the model (Fig. 5). This contour region corresponded to a temperature range between 37 and 39°C and to a time value around 4 days. Moreover, FERH intercalation was improved by

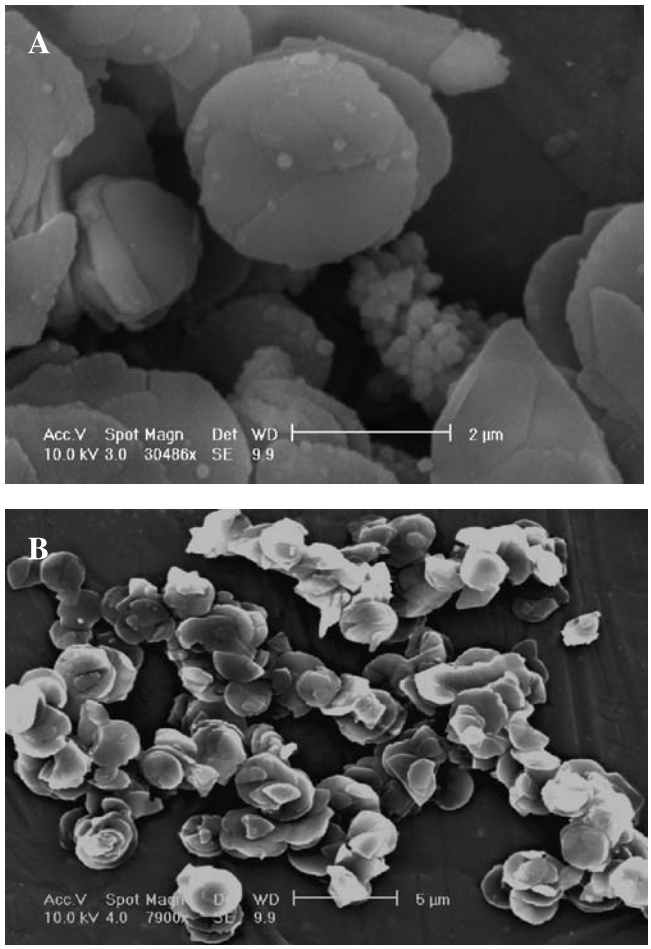

Fig. 4. Scanning electron microscopy pictures of HTlc–FER intercalation compounds (A) and blank HTlc–Cl matrix (B).

increasing time exposure to lower temperatures, and it was decreased at higher temperatures. This behavior can be easily explained if considering that although FERH intercalation kinetics is strongly speeded up by a temperature increase, temperature affects FERH stability; therefore, working for longer times at higher temperatures leads to degradation and to a decrease of intercalation efficiency. On the contrary, at low temperatures, degradation is not particularly fast, and longer times are required to counterbalance the kinetics slacking up. Of course, too low temperatures, although desirable for FERH preservation, should be avoided to not slow down excessively the intercalation reaction. Therefore, improvement of FERH intercalation can be achieved by properly modifying process conditions as earlier suggested. However, pH being a key factor for obtaining a sufficiently high intercalation, FERH stability was investigated looking at several pH and temperature setups as well. The studies were carried out by RP-HPLC. Optimal resolution and peak symmetry were achieved using a mixture of CH_3COOH water solution (pH 3) and acetonitrile (66:34, v/v) as mobile phase. A FERH aqueous solution, injected as a standard, showed a retention time of 4.7 min. A FERH calibration curve ($r^2 > 0.990$) was used to quantify the FERH concentration in buffer solutions. Figure 6A–C showed that FERH degradation increased with temperature and pH. In fact, an evident faster drop of FERH concentration was

Table II. Analysis of Variance of the Quadratic Model for the Intercalation Study Obtained from the RSM Design

Source	Sum of squares	*df*	Mean square	*F* value	Prob > *F*	
Model	217.32	4	54.33	16.50	0.0011	Significant
A	10.97	1	10.97	3.33	0.1108	
B	116.95	1	116.95	35.51	0.0006	
B^2	64.84	1	64.84	19.69	0.0030	
AB	23.92	1	23.92	7.26	0.0309	
Residual	23.05	7	3.29			
Cor total	240.38	11				

RSM: Response surface method.

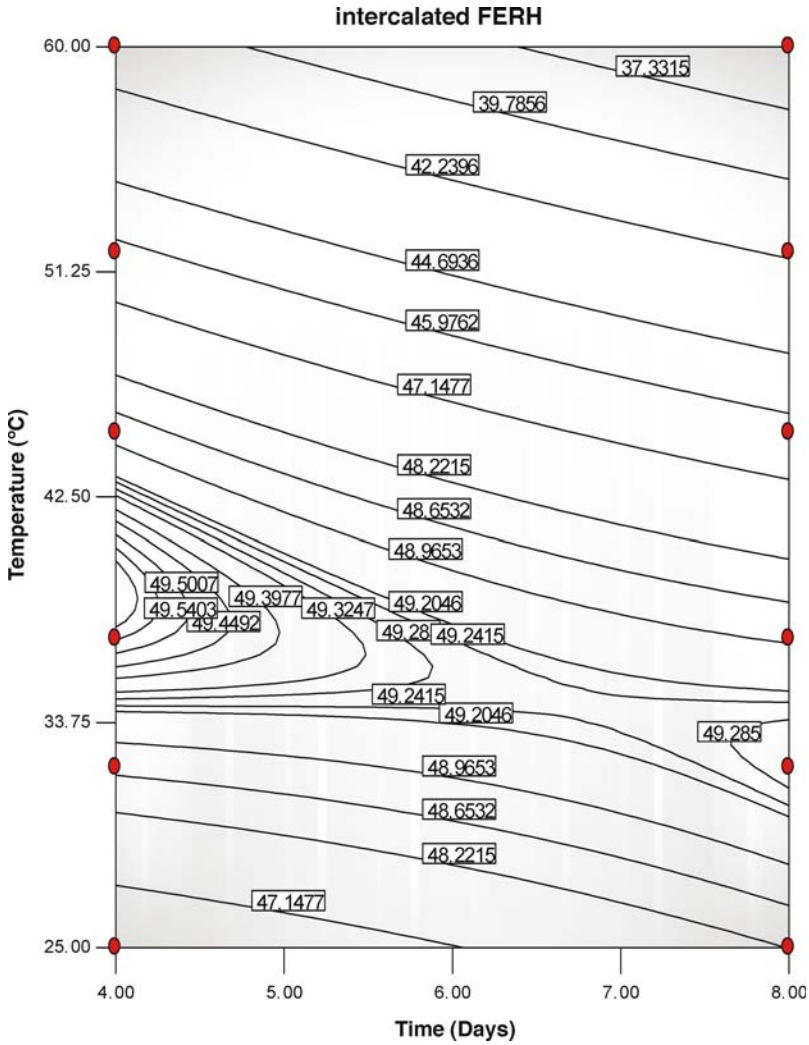

Fig. 5. Contour plot of the % amount of intercalated FERH as function of time and temperature as obtained from the response surface method design.

observed at 37 and 60°C, when pH was increased from 2.2 to 7.4 (Fig. 6B and C). This behavior was not observed at 4°C, as at this temperature, FERH was stable over 220 days, although a drop of about 10% was still recorded at pHs 4 and 7.4 if compared to pH 2.2 (Fig. 6A).

Evaluation of the extent of temperature and pH effects observed during the FERH stability study was performed by a D-optimal design. For this purpose, FERH degradation rate constants k were calculated as previously reported from the Arrhenius plots and were used for the experimental design study. As a consequence of a nonlinear k response to temperature and pH variation, a reduced cubic model was obtained.

$$Y = 0.33 + 1.28X_A + 0.050X_B + 1.13X_A^2 + 0.075X_AX_B + 0.11X_A^2X_B \quad (5)$$

Diagnostic and ANOVA analyses showed a good performance and reliability of the model with high significant terms as shown by the large F values (Table III). A nonsignificant lack of fit and a high correlation with $r^2 > 0.990$ (data not shown) claimed a high efficiency of the model in fitting experimental data. A good agreement was observed between predicted and adjusted r^2 (data not shown).

pH did not directly affect intercalation by itself, but it had a high importance in influencing temperature effect. Evaluation of k surface plot showed an increase of FERH degradation rate when both temperature and pH were increased (Fig. 7). The effect of temperature was by far greater than pH's as from the surface area steepest profile. These findings correlated well with the results from the stability study. In fact, the optimal conditions, indicated by the contour region in which k was minimum, corresponded to low temperature and to low pH values. In this regard, the use of low pHs is desirable to limit the presence of negatively charged species in solution, reducing thus the risk of FERH displacement. Moreover, stability and experimental design studies showed that low pHs slightly reduce FERH degradation rate at higher temperatures, whereas, as previously shown (Fig. 6A), negligible differences occur at low temperatures. This observation was correlated with a higher stability of the undissociated vs. the dissociated form of the compound with temperature. This result confirmed the findings reported earlier (22), which stated a certain FERH stability with pH

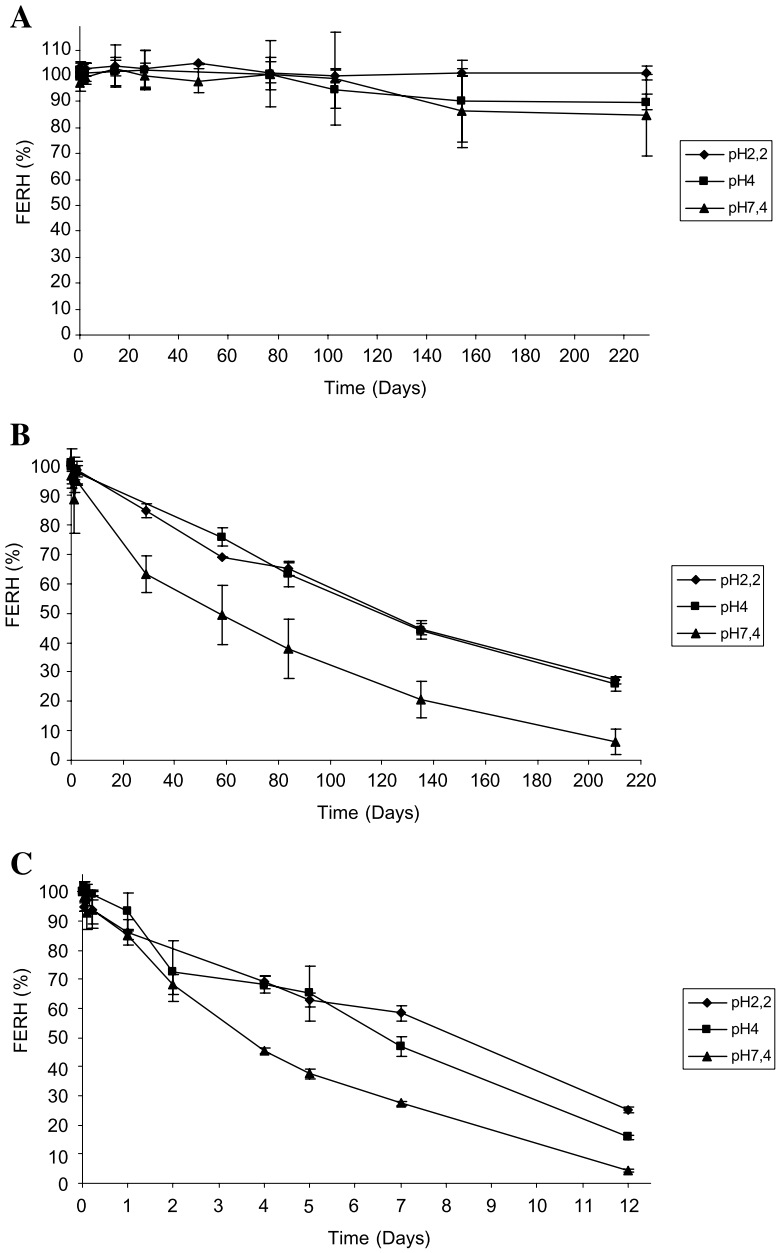

Fig. 6. FERH stability in dependence of pH at 4°C (A), 37°C (B), and 60°C (C).

(3–11) at room and low temperatures (6°C) in proper buffers. Moreover, a pH within FERH pK_a and 7 is desirable, because, as already stated, neutral and basic pHs must be avoided to reduce the amount of negatively charged species, such as OH^-, which compete with FERH during the intercalation process. Besides, the high instability of HTlc below pH 5 put another constrain to the choice of the proper pH value. Therefore, a pH value around 6 was thought to be a good compromise to fulfill all requirements. In fact, being FERH pK_a about 4.5, at pH 6, most of it is present in a dissociated form. Moreover, working at a pH < 7 ensures both requirements: (1) sufficient FERH stability over the period of time investigated and (2) limited presence of competitive species in solution. Of course, additional care has to be taken as far as light effect is concerned. In fact, light exposure is critical to FERH to not impair its structure and its physical–chemical properties. For this reason, all experiments were performed avoiding light exposure.

Evaluation of FERH Degradation

Qualitative analyses of chromatograms and UV profiles were carried out as a consequence of the decrease of FERH content observed during 8 days of intercalation time at 52°C and during days 4 and 8 when intercalation was performed at 60°C. In these cases, the percentage of FERH intercalated was between 35 and 40%, respectively, whereas in all other cases, the FERH content in HTlc–FER was found to be about 48% w/w. To explain this content decrease, the supernatants, collected during the intercalation study reported in Intercalation of FERH into HTlc–Cl, were submitted to RP-HPLC analysis. All chromatograms were

Table III. Analysis of Variance of the Reduced Cubic Model Obtained for the Stability Study from the RSM Design

Source	Sum of squares	*df*	Mean square	*F* value	Prob > *F*	
Block	4.87	2	2.44			
Model	64.44	5	12.89	3640.70	<0.0001	Significant
A	55.87	1	55.87	15,782.54	<0.0001	
B	4.885E−003	1	4.885E−003	1.38	0.2469	
A^2	7.12	1	7.12	2010.97	<0.0001	
AB	0.18	1	0.18	50.94	<0.0001	
A^2B	0.022	1	0.022	6.18	0.0171	
Residual	0.15	41	3.540E−003			
Lack of fit	0.015	3	5.017E−003	1.47	0.2392	Not significant
Pure error	0.13	38	3.423E−003			
Cor total	69.46	48				

RSM: Response surface method.

characterized by a single peak corresponding to FERH at 25, 32, and 37°C for both 4- and 8-day intercalation times. Chromatograms of samples obtained after 4 days at 45°C (Fig. 8A) showed an additional small peak at 7.7 min. This result was interpreted as due to a first degradation product. A similar chromatogram was observed for samples obtained at 45°C after 8 days and at 52°C after 4 days (data not shown). On the contrary, the sample prepared at 52°C for 8 days showed larger and smaller peaks at 7.7- and 12.8-min retention times, respectively, corresponding to possible different degradation products (Fig. 8B). Samples prepared at 60°C, whether at 4 or 8 days, showed similar chromatograms with the two degradation products. However, although the FERH peak was always present in all chromatograms, at 8 days, it was strongly reduced, and the two degradation products turned out to be the main constituents (Fig. 8C). These observations suggest that a remarkable degradation starts at temperatures above 45–50°C, with some additional peaks appearing in the FERH chromatograms. At lower temperatures, these peaks are no longer detectable, confirming thus that performing the process at a temperature below 40°C not only represents the most suitable and the safest working condition but is also capable of insuring a sufficiently high inclusion rate. Comparison of chromatograms obtained from the analysis of supernatants of the FERH intercalation process and the HPLC profile of 4-vinylguaiacol, one of the known FERH degradation products, did not show any matching peak. The reason for this resides either in a possible FERH alternative degradation pathway or in that 4-vinylguaiacol degrades into further byproducts.

CONCLUSIONS

A new potentially useful protocol for an improved FERH intercalation into HTlc matrices is developed.

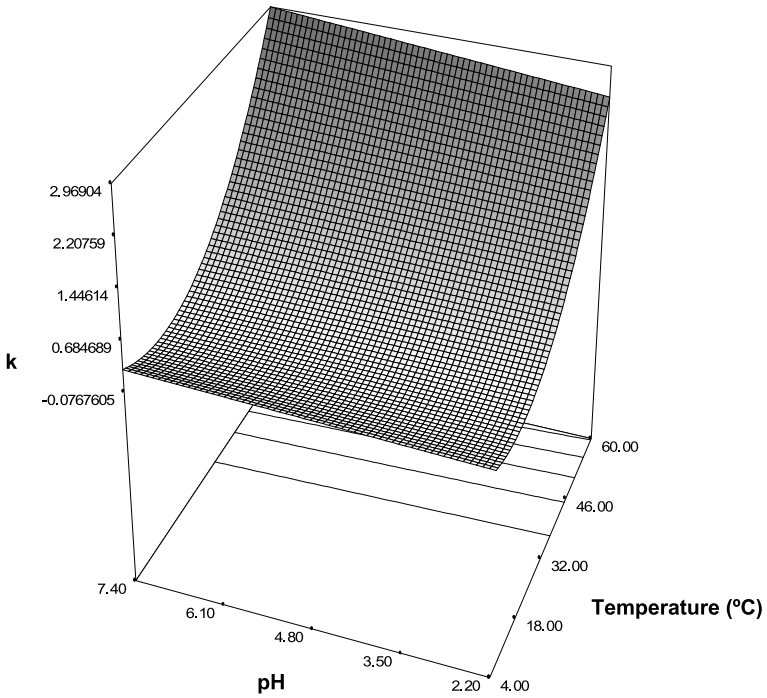

Fig. 7. Response surface plot showing the dependence of the FERH degradation rate constant *k* on temperature and pH.

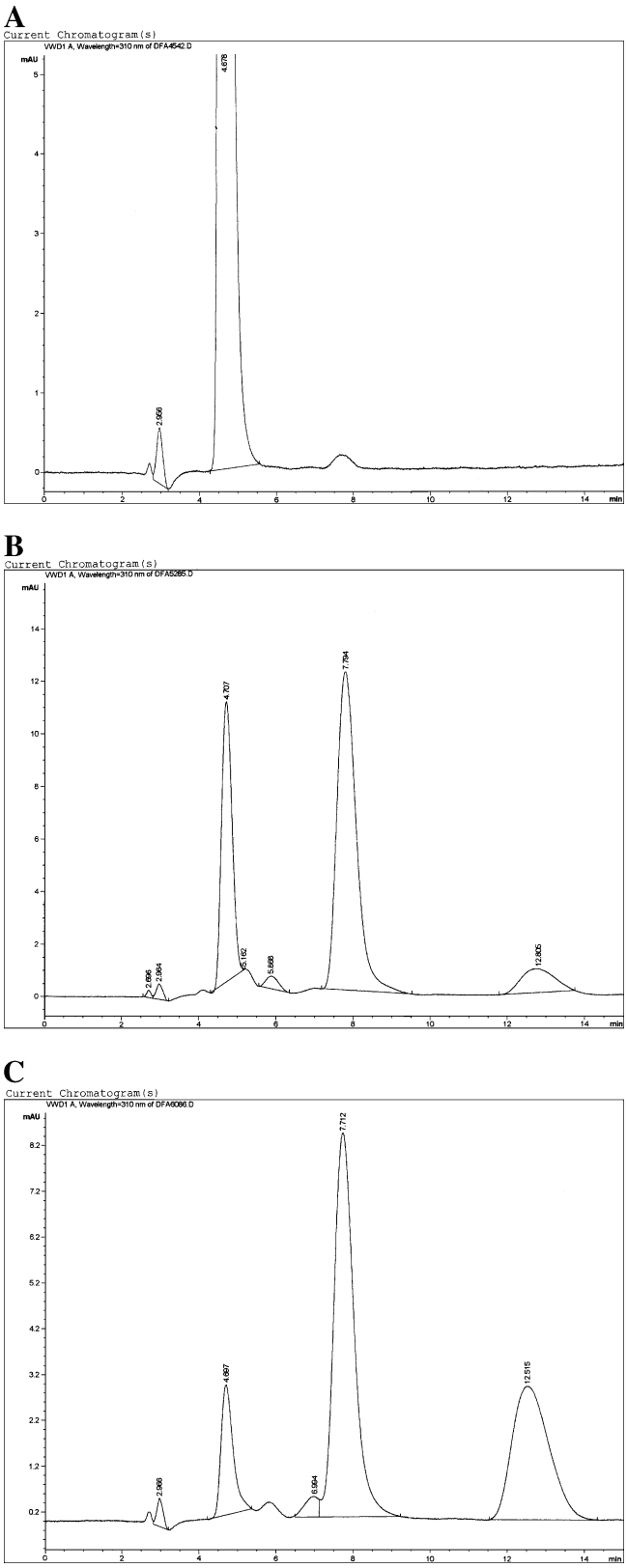

Fig. 8. Chromatograms of the supernatants coming from the intercalation study, collected after 4 days at 45°C (A), after 8 days at 52°C (B), and after 8 days at 60°C (C).

According to the results obtained, the optimal working conditions for FERH intercalation into HTlc–Cl matrices are the following: (1) temperatures between 25 and 40°C, (2) working periods of 4 days, and (3) a pH around 6. The assessment of such conditions should ensure the safety of the inclusion products and improve its intercalation process efficiency. Moreover, the increase of the FERH-intercalated amount enhances its performances and effectiveness upon application *in vivo*. These characteristics may provide a new powerful tool for skin protection over several oxidative stress processes.

ACKNOWLEDGMENTS

This work was supported by the Italian Ministry for Education, University and Research (MIUR)—research programs of national interest.

REFERENCES

1. Z. Wei and Y. W. Shiow. Antioxidant activity and phenolic compounds in selected herbs. *J. Agric. Food Chem.* **49**:5165–5170 (2001).
2. M. Lodovici, F. Guglielmi, M. Meoni, and P. Dolora. Effect of natural phenolic acids on DNA oxidation *in vitro*. *Food Chem. Toxicol.* **39**:1205–1210 (2001).
3. H. S. Ju, X. J. Li, B. L. Zhao, J. W. Hou, Z. W. Han, and W. J. Xin. Scavenging effects of sodium ferulate and 18 h-glycyrrhetic acid on oxygen free radicals. *Acta Pharmacol. Sin.* **11**:466–470 (1990).
4. A. Saija, A. Tomaino, R. LoCascio, D. Trombetta, A. Proteggente, A. De Pasquale, N. Uccella, and F. Bonina. Ferulic and caffeic acids as potential protective agents against photooxidative skin damage. *J. Sci. Food Agric.* **79**:476–480 (1999).
5. E. Graf. Antioxidant potential of ferulic acid. *Free Radic. Biol. Med.* **13**:435–448 (1992).
6. C. Rossi, A. Schoubben, M. Ricci, L. Perioli, V. Ambrogi, L. Zatterini, G. G. Aloisi, and A. Rossi. Intercalation of the radical scavenger ferulic acid in hydrotalcite-like anionic clays. *Int. J. Pharm.* **295**:47–55 (2005).
7. U. Costantino, F. Marmottini, M. Nocchetti, and R. Vivani. New synthetic routes to hydrotalcite-like compounds—characterisation and properties of the obtained materials. *Eur. J. Inorg. Chem.* **10**:1439–1446 (1998).
8. D. Kishore and S. Kannan. Environmentally benign route for isomerization of safrole–hydrotalcite as solid base catalyst. *J. Mol. Catal., A Chem.* **223**:225–230 (2004).
9. S. Narayanan and K. Krishna. Highly active hydrotalcite supported palladium catalyst for selective synthesis of cyclohexanone from phenol. *Appl. Catal., A Gen.* **147**:1253–1258 (1996).
10. J. Orthman, H. Y. Zhu, and G. Q. Lu. Use of anion clay hydrotalcite to remove coloured organics from aqueous solutions. *Sep. Purif. Technol.* **31**:53–59 (2003).
11. S.-Y. Kwak, W. M. Kriven, M. A. Wallig, and J.-H. Choy. Inorganic delivery vector for intravenous injection. *Biomaterials* **25**:5995–6001 (2004).
12. V. Ambrogi, G. Fardella, G. Grandolini, L. Perioli, and M. C. Tiralti. Intercalation compounds of hydrotalcite-like anionic clays with anti-inflammatory agents. II: Uptake of diclofenac for a controlled release formulation. *AAPS PharmSciTech* **3**:E26, 2002 (2002).
13. A. Xu, H. Qi, and W. Shieh. Preparation of stabilized cyclodextrin complexes. U.S. Patent No. 99,172,099 (2001).
14. B. Karmakar, R. M. Vohra, H. Nandanwar, P. Sharma, K. G. Gupta, and R. C. Sobti. Rapid degradation of ferulic acid via 4-vinylguaiacol and vanillin by a newly isolated strain of *Bacillus coagulans*. *J. Biotechnol.* **80**:195–202 (2000).

15. U. Krings, S. Pilawa, C. Theobald, and R. G. Berger. Phenyl propenoic side chain degradation of ferulic acid by *Pycnoporus cinnabarinus*—elucidation of metabolic pathways using [5-2*H*]-ferulic acid. *J. Biotechnol.* **85**:305–314 (2001).
16. M. Brunati, F. Marinelli, C. Bertolini, R. Gandolfi, D. Daffonchio, and F. Molinari. Biotransformations of cinnamic and ferulic acid with actinomycetes. *Enzyme Microb. Technol.* **34**:3–9 (2004).
17. I. McMurrough, D. Madigan, D. Donnely, J. Hurley, A. M. Doyle, G. Hennigan, N. McNultly, and M. R. Smyth. Control of ferulic acid and 4-vinyl guaiacol in brewing. *J. Inst. Brew.* **102**:327–332 (1996).
18. G. P. Rizzi and L. J. Boekley. Observation of ether-linked phenolic products during thermal degradation of ferulic acid in the presence of alcohols. *J. Agric. Food Chem.* **40**:1666–1670 (1992).
19. S. Coghe, K. Benoot, F. Delvaux, B. Verhaegen, and F. R. Delvaux. Ferulic acid release and 4-vinylguaiacol formation during brewing and fermentation: indications for feruloyl esterase activity in *Saccharomyces cerevisiae*. *J. Agric. Food Chem.* **52**:602–608 (2004).
20. R. Dorfner, T. Ferge, A. Kettrup, R. Zimmermann, and C. Yeretzian. Real-time monitoring of 4-vinylguaiacol, guaiacol, and phenol during coffee roasting by resonant laser ionization time-of-flight mass spectrometry. *J. Agric. Food Chem.* **51**:5768–5773 (2003).
21. G. X. Pan, L. Spencer, and G. J. Leary. Reactivity of ferulic acid and its derivatives toward hydrogen peroxide and peracetic acid. *J. Agric. Food Chem.* **47**:3325–3331 (1999).
22. M. Friedman and H. S. Jürgens. Effect of pH on the stability of plant phenolic compounds. *J. Agric. Food Chem.* **48**:2101–2110 (2000).
23. W. T. Reichle. Synthesis of anionic clay minerals (mixed metal hydroxides, hydrotalcite). *Solid State Ionics* **22**:135–141 (1986).
24. S. Miyata. Anion-exchange properties of hydrotalcite-like compounds: characterization and properties of the obtained materials. *Clay Miner.* **31**:305–311 (1983).
25. N. T. Whilton, P. J. Vickers, and S. Mann. Bioinorganic clays: synthesis and characterization of amino- and polyamino acid intercalated layered double hydroxides. *J. Mater. Chem.* **7**:1623–1629 (1997).